Increasing efficiency of a linear-optical quantum gate using electronic feed-forward

Martina Miková, Helena Fikerová, Ivo Straka, Michal Mičuda, Jaromír Fiurášek, Miroslav Ježek, and Miloslav Dušek
Department of Optics, Faculty of Science, Palacky University, 17. listopadu 12, CZ-771 46 Olomouc, Czech Republic
(Received 4 November 2011; published 4 January 2012)

We have successfully used fast electronic feed-forward to increase the probability of success of a linear optical implementation of a programmable phase gate from 25% to its theoretical limit of 50%. The feed-forward applies a conditional unitary operation, which changes the incorrect output states of the data qubit to the correct ones. The gate itself rotates an arbitrary quantum state of the data qubit around the z axis of the Bloch sphere with the angle of rotation being fully determined by the state of the program qubit. The gate implementation is based on fiber optics components. Qubits are encoded into spatial modes of single photons. The signal from the feed-forward detector is led directly to a phase modulator using only a passive voltage divider. We have verified the increase of the probability of success and characterized the gate operation by means of quantum process tomography. We have demonstrated that the use of feed-forward affects neither the process fidelity nor the output-state fidelities.

DOI: 10.1103/PhysRevA.85.012305 PACS number(s): 03.67.Lx, 42.50.Ex

I. INTRODUCTION

Linear-optical architectures are some of the most prominent platforms for realizing protocols of quantum information processing [1,2]. They are experimentally feasible and work directly with photons without the necessity of transfering the quantum state of a photonic qubit into another quantum system, such as an ion. The latter feature is quite convenient because photons are good carriers of information for communication purposes. Linear-optical quantum gates achieve the nonlinearity necessary for the interaction between qubits by means of the nonlinearity of quantum measurement. Unfortunately, quantum measurement is not only nonlinear but also probabilistic. Therefore, linear-optical implementations of quantum gates are mostly probabilistic, too—their operation sometimes fails. Partly, this is a fundamental limitation, but in many cases when data qubits appear in an improper state after the measurement on an ancillary system, they can still be corrected by applying a proper unitary transformation which depends only on the measurement result. In these situations, implementation of feed-forward can increase the probability of success of the gate [3,4]. In the present paper, we apply this approach to a linear-optical programmable quantum gate.

Most conventional computers use fixed hardware, and different tasks are performed using different software. This concept can be applied, in principle, to quantum computers as well: The unitary operation executed by the gate can be determined by some kind of a program. However, in 1997 Nielsen and Chuang [5] showed that an n-qubit quantum register can perfectly encode at most 2^n distinct quantum operations. Although this bound rules out perfect universally programmable quantum gates (even unitary transformations on only one qubit form a group with uncountably many elements), it is still possible to construct approximate or probabilistic programmable quantum gates and optimize their performance for a given size of the program register. Such gates can either operate deterministically, but with some noise added to the output state [6], or operate probabilistically and error free [7–9]. Combinations of these regimes are also possible.

A probabilistic programmable phase gate was proposed by Vidal, Masanes, and Cirac [8]. It carries out rotation of a single-qubit state along the z axis of the Bloch sphere. The angle of rotation (or the phase shift) is programmed into the state of a single-qubit program register. It is worth noting that an exact specification of an angle of rotation would require infinitely many classical bits, but here the information is encoded into a single qubit only. The price is that the success probability of such a gate is limited by 50% [10]. The programmable phase gate was experimentally implemented for the first time in 2008 [11]. However, the success probability of that linear-optical implementation reached only 25%. In the present paper, we will show how to increase the probability of success of this scheme to its quantum mechanical limit of 50% by means of electronic feed-forward [12].

II. THEORY

The programmable phase gate works with a data qubit and a program qubit. The program qubit contains information about the phase shift ϕ encoded in the following way:

$$|\phi\rangle_P = \frac{1}{\sqrt{2}}(|0\rangle_P + e^{i\phi}|1\rangle_P). \tag{1}$$

The gate performs a unitary evolution of the data qubit, which depends on the state of the program qubit:

$$U(\phi) = |0\rangle_D\langle 0| + e^{i\phi}|1\rangle_D\langle 1|. \tag{2}$$

Without loss of generality, we can consider only pure input states of the data qubit:

$$|\psi_{\text{in}}\rangle_D = \alpha|0\rangle_D + \beta|1\rangle_D. \tag{3}$$

The output state of the data qubit reads

$$|\psi_{\text{out}}\rangle_D = \alpha|0\rangle_D + e^{i\phi}\beta|1\rangle_D. \tag{4}$$

The programmable phase gate can be experimentally implemented with the optical setup shown in Fig. 1. Each qubit is represented by a single photon which may propagate in two optical fibers. The basis states $|0\rangle$ and $|1\rangle$ correspond to the presence of the photon in the first or the second fiber, respectively. When restricted only to the cases when a single photon emerges in each output port, the conditional

two-photon output state reads (the normalization reflects the fact that the probability of this situation is $\frac{1}{2}$):

$$\frac{1}{\sqrt{2}}(\alpha|0\rangle_D \otimes |0\rangle_P + \beta e^{i\phi}|1\rangle_D \otimes |1\rangle_P)$$
$$= \frac{1}{2}[(\alpha|0\rangle_D + \beta e^{i\phi}|1\rangle_D)\otimes|+\rangle_P$$
$$+ (\alpha|0\rangle_D - \beta e^{i\phi}|1\rangle_D)\otimes|-\rangle_P],$$

where $|\pm\rangle_P = \frac{1}{\sqrt{2}}(|0\rangle_P \pm |1\rangle_P)$. If we make a measurement on the program qubit in the basis $\{|\pm\rangle_P\}$, then also the output state of the data qubit collapses into one of the two following states according to the result of the measurement: $|\psi_{\text{out}}\rangle_D = \alpha|0\rangle_D \pm \beta e^{i\phi}|1\rangle_D$. If the measurement outcome is $|+\rangle_P$, then the unitary transformation $U(\phi)$ has been applied to the data qubit. If the outcome is $|-\rangle_P$, then $U(\phi+\pi)$ has been executed; that is, the state acquired an extra π phase shift. This phase shift is compensated for via a fast electro-optical modulator which applies a corrective phase shift of $-\pi$ (in practice we apply a phase shift of π, which is equivalent).

III. EXPERIMENT

The scheme of the setup is shown in Fig. 1. Pairs of photons are created by type II collinear frequency-degenerate spontaneous parametric down conversion (SPDC) in a 2-mm-long beta barium borate (BBO) crystal pumped by a diode laser (Coherent Cube) at 405 nm [13]. The photons from each pair are separated by a polarizing beam splitter and coupled into single-mode fibers. Using fiber polarization controllers, the same polarizations are set on both photons. By means of fiber couplers and electro-optical phase modulators, the required input states of the program and data qubits are prepared. To prepare state (1) of the program qubit, a fiber coupler (FC) with a fixed splitting ratio of 50:50 is used. An arbitrary state of the data qubit (3) is prepared using an electronically controlled variable ratio coupler (VRC). All phase modulators employed (EO Space) are based on the linear electro-optic effect in lithium niobate. Their half-wave voltages are about 1.5 V. These phase modulators (PMs) exhibit relatively high dispersion. Therefore, one PM is placed in each interferometer arm in order to compensate for dispersion effects. Because the overall phase of a quantum state is irrelevant, it is equivalent to apply a phase shift of either φ to $|1\rangle$ or $-\varphi$ to $|0\rangle$.

The gate itself consists of the exchange of two rails of input qubits and the measurement on the data qubit (see Fig. 1). The measurement in basis $\{|\pm\rangle\}$ is accomplished by a fiber coupler with fixed splitting ratio 50:50 and two single-photon detectors. In this experiment, we use single-photon counting modules (Perkin-Elmer) based on actively quenched silicon avalanche photodiodes. Detectors D_{p0}, D_{d0}, and D_{d1} belong to a quad module SPCM-AQ4C (total efficiencies 50–60%, dark counts 370–440 s^{-1}, response time 33–40 ns). A single module SPCM AQR-14FC is used as D_{p1}, serving for the feed-forward, because of its faster response (total efficiency about 50%, dark counts 180 s^{-1}, response time 17 ns). The output of the detector is a 31-ns-long 5-V pulse.

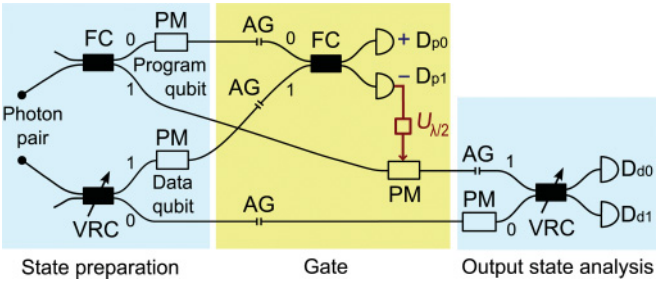

FIG. 1. (Color online) Scheme of the experiment. FC, fiber couplers; VRC, variable ratio couplers; PM, phase modulators; AG, air gaps; and D, detectors.

To implement the feed-forward, the signal from detector D_{p1} is led to a passive voltage divider, in order to change the 5-V voltage level to about 1.5 V (necessary for the phase shift of π) and then directly to the phase modulator. The coaxial jumpers are as short as possible. The total delay including the time response of the detector is 20 ns. To compensate for this delay, photon wave packets representing data qubits are retarded by fiber delay lines (a coil of fiber approximately 8 m long in each interferometer arm). The timing of the feed-forward pulse and the photon arrival were precisely tuned. The coherence time of the photons created by our SPDC source is only several hundreds of femtoseconds.

The right-most block in Fig. 1 enables us to measure the data qubit at the output of the gate in an arbitrary basis. These measurements are necessary to the evaluate performance of the gate.

The whole experimental setup is formed by two Mach-Zehnder interferometers (MZIs). The lengths of the arms of the shorter MZI (the upper interferometer in Fig. 1) are about 10.5 m. The lengths of the arms of the longer one (the lower interferometer in Fig. 1) are about 21.5 m. To balance the arm lengths, we use motorized air gaps with adjustable lengths. Inside the air gaps, polarizers and wave plates are also mounted. They serve for accurate setting of polarizations of the photons (to obtain high visibilities, the polarizations in both arms of each MZI must be the same).

To reduce the effect of the phase drift caused by fluctuations of temperature and temperature gradients, we apply both passive and active stabilization. The experimental setup is covered by a shield minimizing air flux around the components and both delay fiber loops are wound on an aluminium cylinder, which is thermally isolated. Besides, an active stabilization is performed after every 3 s of measurement. It measures intensities for phase shifts 0 and $\pi/2$, and if necessary it calculates the phase compensation needed and applies corresponding corrective voltage to the phase modulator. Consequently, the precision of phase setting during the measurement period is better than $\pi/200$. For the stabilization purposes, we use a laser diode at 810 nm. To ensure the same spectral range, both the laser beam and SPDC-generated photons pass through the same band-pass interference filter (spectral FWHM 2 nm, Andover). During active stabilization, the source is automatically switched from SPDC to the laser diode.

The aim of our experiment is to demonstrate the function of feed-forward. The setup is not optimized for minimal loss. Notice, however, that the additional losses due to the delay lines are negligible (10 m of fiber add about 0.03 dB at 810 nm).

IV. RESULTS

Any quantum operation can be fully described by a completely positive (CP) map. According to the Jamiołkowski-Choi isomorphism, any CP map can be represented by a positive-semidefinite operator χ on the tensor product of input and output Hilbert spaces $\mathcal{H}_{\rm in}$ and $\mathcal{H}_{\rm out}$ [14,15]. The input state $\rho_{\rm in}$ transforms according to

$$\rho_{\rm out} = {\rm Tr}_{\rm in}\left[\chi\left(\rho_{\rm in}^{T}\otimes I_{\rm out}\right)\right].$$

Combinations of different input states with measurements on the output quantum system represent effective measurements performed on $\mathcal{H}_{\rm in}\otimes\mathcal{H}_{\rm out}$. A proper selection of the input states and final measurements allows us to reconstruct matrix χ from measured data using the maximum likelihood (ML) estimation technique [16,17].

For each phase shift, that is, for a fixed state of the program qubit, we used six different input states of the data qubit, namely $|0\rangle,|1\rangle,|\pm\rangle=(|0\rangle\pm|1\rangle)/\sqrt{2}$, and $|\pm i\rangle=(|0\rangle\pm i|1\rangle)/\sqrt{2}$. For each of these input states, the state of the data qubit at the output of the gate was measured in three different measurement bases, $\{|0\rangle,|1\rangle\},\{|\pm\rangle\}$, and $\{|\pm i\rangle\}$. Each time, we simultaneously measured two-photon coincidence counts between detectors D_{p0} and D_{d0}, D_{p0} and D_{d1}, D_{p1} and D_{d0}, and D_{p1} and D_{d1} in twelve 3-s intervals [18]. The unequal detector efficiencies were compensated for by proper rescaling of the measured coincidence counts. From these data, we have reconstructed Choi matrices describing the functioning of the gate for several different phase shifts. In Figs. 2 and 3, there are examples of the Choi matrices for the gates for $\phi=\pi/2$ and $\phi=\pi$, respectively.

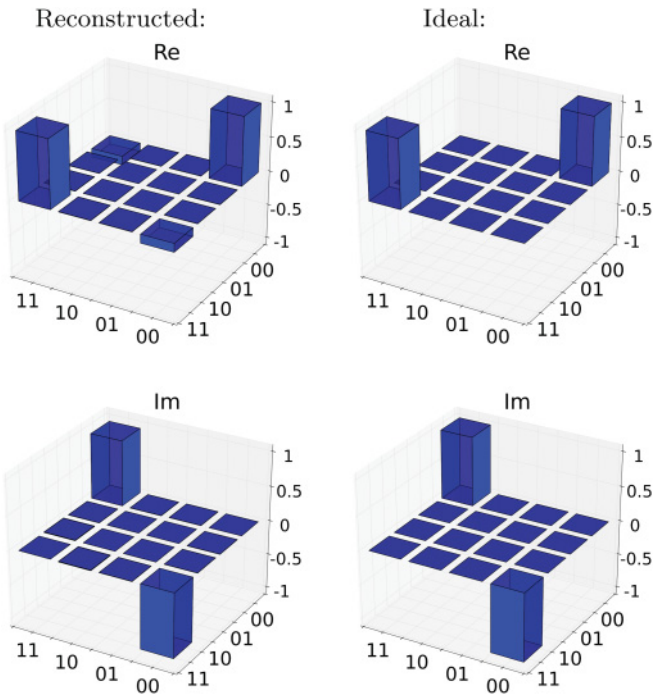

FIG. 2. (Color online) Choi matrix for the gate with the feed-forward when $\phi=\pi/2$ is encoded into the program qubit. The left top panel shows the real part of the reconstructed process matrix, and the left bottom one displays its imaginary part. The two right panels show the real and imaginary parts of the ideal matrix.

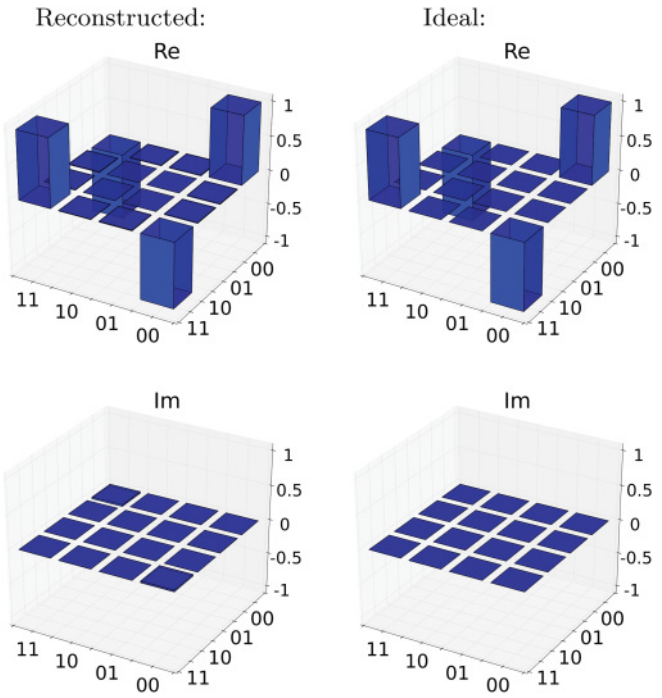

FIG. 3. (Color online) Choi matrix for the gate with the feed-forward when $\phi=\pi$ is encoded into the program qubit. The left top panel shows the real part of the reconstructed process matrix, and the left bottom one displays its imaginary part. The two right panels show the real and imaginary parts of the ideal matrix.

To quantify the quality of gate operation, we have calculated the process fidelity. If $\chi_{\rm id}$ is a one-dimensional projector, then the common definition of the process fidelity is

$$F_{\chi} = {\rm Tr}[\chi\,\chi_{\rm id}]/({\rm Tr}[\chi]{\rm Tr}[\chi_{\rm id}]).$$

Here $\chi_{\rm id}$ represents the ideal transformation corresponding to our gate. In particular,

$$\chi_{\rm id} = \sum_{i,j=0,1} |i\rangle\langle j|\otimes U|i\rangle\langle j|U^{\dagger},$$

where U stands for the unitary operation (2) applied by the gate.

We have also reconstructed density matrices of the output states of the data qubit corresponding to all input states and calculated fidelities and purities of the output states. The fidelity of output state $\rho_{\rm out}$ is defined as $F=\langle\psi_{\rm out}|\rho_{\rm out}|\psi_{\rm out}\rangle$, where

TABLE I. Process fidelities (F_{χ}), average ($F_{\rm av}$) and minimal ($F_{\rm min}$) output-state fidelities, and average ($\mathcal{P}_{\rm av}$) and minimal ($\mathcal{P}_{\rm min}$) output-state purities for different phases (ϕ) *with* feed-forward ($p_{\rm succ}=50\,\%$).

ϕ	F_{χ}	$F_{\rm av}$	$F_{\rm min}$	$\mathcal{P}_{\rm av}$	$\mathcal{P}_{\rm min}$
0	0.976	0.985	0.970	0.974	0.947
$\pi/6$	0.977	0.986	0.972	0.975	0.951
$\pi/3$	0.977	0.985	0.970	0.975	0.943
$\pi/2$	0.974	0.983	0.973	0.975	0.953
$2\pi/3$	0.978	0.987	0.962	0.988	0.961
$5\pi/6$	0.972	0.981	0.953	0.974	0.944
π	0.980	0.987	0.975	0.977	0.961

TABLE II. Process fidelities (F_χ), average (F_{av}) and minimal (F_{min}) output-state fidelities, and average ($\mathcal{P}_{\text{av}}$) and minimal ($\mathcal{P}_{\text{min}}$) output-state purities for different phases (ϕ) *without* feed-forward ($p_{\text{succ}} = 25\%$).

ϕ	F_χ	F_{av}	F_{min}	$\mathcal{P}_{\text{av}}$	$\mathcal{P}_{\text{min}}$
0	0.977	0.985	0.973	0.975	0.953
$\pi/6$	0.975	0.985	0.972	0.973	0.949
$\pi/3$	0.988	0.989	0.971	0.980	0.946
$\pi/2$	0.979	0.986	0.976	0.976	0.957
$2\pi/3$	0.981	0.989	0.966	0.982	0.935
$5\pi/6$	0.974	0.984	0.961	0.976	0.947
π	0.979	0.986	0.977	0.978	0.960

$|\psi_{\text{out}}\rangle = U|\psi_{\text{in}}\rangle$ with $|\psi_{\text{in}}\rangle$ being the (pure) input state. The purity of the output state is defined as $\mathcal{P} = \text{Tr}[\rho_{\text{out}}^2]$. If the input state is pure, the output state is expected to be pure as well.

Table I shows process fidelities for seven different phase shifts. It also shows the average and minimal values of output-state fidelities and average and minimal purities of output states. Fidelities and purities are averaged over six output states corresponding to six input states described above. Also, the minimum values are related to these sets of states. Statistical errors are estimated to be less than 0.005 for process fidelities and purities and less than 0.01 for output-state fidelities and purities. Deviations of the experimental values from the ideal ones are mainly due to imperfections in splitting-ratio settings, phase fluctuations, polarization misalignment, and partial distinguishability of the photons in a pair.

To evaluate how the feed-forward affects the performance of the gate, we have also calculated process fidelities, output-state fidelities, and output-state purities for the cases when the feed-forward was not active. It means that we have selected only the situations when detector D_{p0} (corresponding to $|+\rangle_P$) clicked and no corrective action was needed (as in Ref. [11]). Coincidences were measured between detectors D_{p0} and D_{d0} and between D_{p0} and D_{d1} only. The total coincidence rate (44 coincidences per second on average) was half in comparison with the sum of all conclusive-result rates in the case with feed-forward (88 coincidences per second in average). The values of fidelities and purities are displayed in Table II. One can see that there is no substantial difference between the operation *with* feed-forward (success probability 50%) and *without* feed-forward (success probability 25%). In particular, the process fidelity in the case with the feed-forward, averaged over all seven phases, is $F_\chi^{\text{with}} = 0.976 \pm 0.003$ and the average process fidelity in the case without the feed-forward is $F_\chi^{\text{without}} = 0.979 \pm 0.005$.

V. CONCLUSIONS

We have implemented a reliable and relatively simple electronic feed-forward system which is fast and which does not require high voltage. We employed this technique to double the probability of success for a programmable linear-optical quantum phase gate. We showed that the application of feed-forward does not affect substantially either the process fidelity or the output-state fidelities. Beside the improvement of efficiency of linear-optical quantum gates, this feed-forward technique can be used for other tasks, such as quantum teleportation experiments or minimal disturbance measurement.

ACKNOWLEDGMENTS

The authors thank Lucie Čelechovská for her advice and for her help in the preparatory phase of the experiment. This work was supported by the Czech Science Foundation (202/09/0747), Palacky University (PrF-2011-015), and the Czech Ministry of Education (MSM6198959213, LC06007).

[1] P. Kok, W. J. Munro, K. Nemoto, T. C. Ralph, J. P. Dowling, and G. J. Milburn, Rev. Mod. Phys. **79**, 135 (2007).
[2] E. Knill, R. Laflamme, and G. J. Milburn, Nature (London) **409**, 46 (2001).
[3] F. Sciarrino, M. Ricci, F. De Martini, R. Filip, and L. Mišta Jr., Phys. Rev. Lett. **96**, 020408 (2006).
[4] R. Prevedel, P. Walther, F. Tiefenbacher, P. Bohl, R. Kaltenbaek, T. Jennewein, and A. Zeilinger, Nature (London) **445**, 65 (2007).
[5] M. A. Nielsen and I. L. Chuang, Phys. Rev. Lett. **79**, 321 (1997).
[6] M. Hillery, M. Ziman, and V. Bužek, Phys. Rev. A **73**, 022345 (2006).
[7] M. Hillery, V. Bužek, and M. Ziman, Phys. Rev. A **65**, 022301 (2002).
[8] G. Vidal, L. Masanes, and J. I. Cirac, Phys. Rev. Lett. **88**, 047905 (2002).
[9] M. Hillery, M. Ziman, and V. Bužek, Phys. Rev. A **69**, 042311 (2004).
[10] By increasing the number of program bits in a semiclassical deterministic case, one increases the precision, and by increasing the number of program qubits in a quantum probabilistic case, one increases the probability of success (see also Ref. [9]).
[11] M. Mičuda, M. Ježek, M. Dušek, and J. Fiurášek, Phys. Rev. A **78**, 062311 (2008).
[12] The success probabilities discussed here do not include signal attenuation due to technological losses.
[13] M. Ježek, I. Straka, M. Mičuda, M. Dušek, J. Fiurášek, and R. Filip, Phys. Rev. Lett. **107**, 213602 (2011).
[14] A. Jamiołkowski, Rep. Math. Phys. **3**, 275 (1972).
[15] M.-D. Choi, Linear Algebr. Appl. **10**, 285 (1975).
[16] M. Ježek, J. Fiurášek, and Z. Hradil, Phys. Rev. A **68**, 012305 (2003).
[17] M. G. A. Paris and J. Řeháček (Editors), *Quantum State Estimation*, Lecture Notes in Physics 649 (Springer, Berlin, 2004).
[18] These output coincidence rates sum up to about 88 coincidences per second.